Journal of Applied Polymer Science

Improved miscibility of low-density polyethylene/chitosan blends through variation in the compounding length

Yi Min Tan,[1] Szu Hui Lim,[2] Bee Yen Tay,[2] Mun Wai Lee,[3] Eng San Thian[1]

[1]Department of Mechanical Engineering, National University of Singapore, 9 Engineering Drive 1, Singapore 117576, Singapore
[2]Forming Technology Group, Singapore Institute of Manufacturing Technology, 71 Nanyang Drive, Singapore 638075, Singapore
[3]Food Innovation and Resource Centre, Singapore Polytechnic, 500 Dover Road, Singapore 139651, Singapore
Correspondence to: E. S. Thian (E-mail: mpetes@nus.edu.sg)

ABSTRACT: Synthetic biopolymer blends are gaining interest in the packaging industry because the incorporation of natural materials imparts biodegradable properties to films. In this study, polyethylene/chitosan (chitosan) films with thicknesses of about 0.3 ± 0.01 mm were fabricated via compression molding. The effects of the variation in the length of compounding as a function of the length/diameter (l/d) ratio (15:1, 30:1, 45:1, 60:1, and 75:1) were investigated. The experimental results show that a higher degree of miscibility of the blends was achieved with increasing compounding length; this led to improved mechanical properties in the films, and this was verified by the statistical analysis of data with the analysis of variance procedure. The tensile strength (TS) increased by about 25%, whereas the elongation at break (E_{break}) increased by twofold. Films fabricated from blends compounded with an l/d ratio of 60:1 had the highest TS and E_{break} values, and the TS was comparable to that of low-density polyethylene films. © 2016 Wiley Periodicals, Inc. J. Appl. Polym. Sci. **2016**, *133*, 43796.

KEYWORDS: blends; films; packaging

Received 21 October 2015; accepted 12 April 2016
DOI: 10.1002/app.43796

INTRODUCTION

Polyethylene (PE) is a commonly used polyolefin; it is widely used in our daily lives because of its good processability, low production cost, and versatility in applications. With its superior properties over other materials for packaging, PE is used extensively in flexible packaging.[1] However, the disposal of PE packaging for short-term applications after use has led to an increase in waste and causes long-term environmental pollution as synthetic polymers are very resistant to degradation and remain in the environment for a very long time.[2] Therefore, a rising awareness and concern for the environment have led to studies on the development of alternative materials with improved biodegradability that are more environmentally friendly.

A method for obtaining new combinations of materials with useful properties is the blending of synthetic materials with natural materials that are biodegradable.[3–6] Blending allows the functional properties of the materials to be enhanced for a broader range of potential applications. Furthermore, as synthetic polymers are commonly available and have a low cost of production, polymer blends are gaining importance because of their favorable balance among their properties, cost, and environmental requirements.[7]

Chitosan, a linear polysaccharide consisting of ^{1,4}-linked 2-amino-deoxy-β-D-glucan, is the *N*-deacetylated derivative of chitin. Chitosan is a renewable raw material commonly found in nature, and it is the second most abundant natural polysaccharide after cellulose. As a natural polysaccharide, chitosan has immense potential for use as a packaging material because of its unique antimicrobial and antifungal properties against many bacteria, filamentous fungi, and yeasts; it is also nontoxic, biocompatible, and biodegradable.[8–10] Hence, the blending of PE with chitosan can incorporate the biodegradability and antimicrobial properties of chitosan into PE for the development of films with better cost–performance ratios.

Because synthetic polymers are hydrophobic and natural polymers are hydrophilic in nature, limited miscibility is a significant factor that affects the mechanical properties in the resulting blend. To obtain good mechanical properties in polymer films, it is crucial to improve the interfacial compatibility and miscibility between chitosan and the PE matrix. Studies have been conducted with the inclusion of polymers grafted with maleic anhydride as compatibilizers into the blend during processing for better interfacial adhesion.[11–13] Quiroz-Castillo *et al.*[3] reported that the use of polyethylene-*graft*-maleic anhydride (PEgMA) as a compatibilizer improved the processability,

compatibility, and mechanical properties of a PE/chitosan mixture. Films with 20 wt % chitosan were obtained compared to films formed without the use of PEgMA.[14] In another investigation by Del Castillo-Castro *et al.*,[12] when 5 wt % PEgMa was added to a PE/polyaniline blend, an increase in the elongation at break (E_{break}) from 93.7 to 243% was observed with an indication of a strengthening at the filler–matrix interfacial region from morphological analysis.

In addition to the incorporation of compatibilizers to improve the properties of polymer blends, good mixing during the compounding process is necessary for the better blending of chitosan and PE to achieve favorable properties. The even distribution of chitosan and compatibilizers in the blend will stabilize the interactions at the polymer interfaces and lead to a reduction in the pore ratio.[15] The successful dispersion of chitosan is also needed to improve the stress-transfer efficiency at the polymer interfaces to obtain enhanced mechanical properties in blend films. Despite studies conducted with the incorporation of compatibilizers for better interfacial adhesion, mixing studies involving PE/chitosan have not been done. Vasile *et al.*[16] melt-processed low-density polyethylene (LDPE) and blends with chitosan with the use of a Brabender mixer at 115 °C and 60 rpm for 10 min. Martínez-Camacho *et al.*[14] formulated LDPE/chitosan blends with a monospindle extrusion machine with one set of conditions (145 and 150 °C, 45 rpm, 2 min). Quiroz-Castillo *et al.*[3] extruded blends of LDPE and chitosan at 130 and 140 °C at a speed of 40 rpm. None of these researchers reported how their conditions were selected.

Because the processing parameters during compounding, extrusion, and molding have effects on the tensile properties and morphologies of the polymer blends,[5] the objective of this study was to enhance the miscibility of PE/chitosan blends through variations in the compounding length as a function of the length/diameter (l/d) ratio (15:1, 30:1, 45:1, 60:1, and 75:1) to achieve improvements in the mechanical properties of the fabricated films. In this study, LDPE was blended with chitosan, a natural biodegradable polymer, with PEgMA as the compatibilizer. The effects of the variation in the compounding length on the morphology, chemical bonding, percentage crystallinity (X_c), and thermal, optical, and mechanical properties of the films were investigated. An increase in the length of compounding during the mixing of the PE/chitosan blends in the fabrication of the films led to increased miscibility and X_c in the films and improved mechanical properties. The chemical, thermal, and optical properties of the PE/chitosan blend films were also maintained.

EXPERIMENTAL

Materials

Powder chitosan with a medium molecular weight (190–310 kDa) and a deacetylation degree of 75–85%, PEgMA (0.85 wt % maleic anhydride), and food-grade glycerol were purchased from Sigma-Aldrich. Commercial-grade LDPE was obtained from Lotte Chemical Titan (M) Sdn. Bhd.

Polymer Processing and the Fabrication of the Films

The PE/chitosan blends were prepared by the mixing of LDPE with chitosan powder. Glycerol was used as a plasticizer for chitosan, as it has good plasticizing power, is nontoxic, and has fairly stable thermal properties.[6] PEgMA was also added as a compatibilizer for interfacial adhesion between LDPE and chitosan. Before mixing, the chitosan powder was dried in an oven for 24 h at 80 °C.

We prepared PE/chitosan blends with a weight ratio of 80/20 by first mixing the chitosan powder with glycerol using a constant weight ratio of 2:1; this was followed by the mixing of the plasticized chitosan with LDPE and 10 wt % PEgMA (amount based on that of chitosan). The blends were extruded by a Haake Force Feeder MiniLab compounder equipped with corotating twin screws ($l = 110$ mm, $d = 5/10$ mm conical). The compounding was carried out at a rotor speed of 50 rpm at 130 °C. To study the effect of the variation in compounding length on the miscibility and mechanical properties of the fabricated films, the PE/chitosan blends were extruded with l/d ratios of 15:1, 30:1, 45:1, 60:1, and 75:1 through the compounder. The blends were classified as PEChi15:1, PEChi30:1, PEChi45:1, PEChi60:1, and PEChi75:1, respectively, with the numbers corresponding to the l/d ratio used for compounding.

The polymer pellets obtained from the compounding process were compression-molded in a Lauffer transfer press for 10 min at 115 °C under a pressure of 150 N/m^2. After pressing, the fabricated films were cooled to room temperature for characterization.

Fourier Transform Infrared (FTIR) Spectra

The IR spectra of all of the PE/chitosan blend films were obtained with an FTIR spectrometer (model Bruker Vertex 80v) in the attenuated total reflectance mode. The film samples were positioned on the sampling stage in direct contact with the optical element for analysis. The background scan and FTIR sample spectra were recorded within the wave-number range 600–4000 cm^{-1} in the transmittance mode. A total of 32 scans were accumulated with a resolution of 4 cm^{-1}.

Thermogravimetric Analysis (TGA)

The thermal stability of the blend films was evaluated via TGA with a TGA Q500 (TA Instruments). Samples of about 6 mg were placed into a standard aluminum pan and heated from 24 to 900 °C at 10 °C/min with a nitrogen air flow at 60 mL/min.

Differential Scanning Calorimetry (DSC) Analysis

The thermal properties of the blend films were evaluated with a differential scanning calorimeter (TA Instruments). Samples of about 5 mg were cut into small pieces from a sample specimen and packed into aluminum pans, crimped closed, and sealed with a DSC sample press. Each sample was heated from 24 to 250 °C at a heating rate of 5 °C/min. Nitrogen was used as the purge gas. The melting temperature (T_m), heat of fusion (ΔH_f), and X_c values of LDPE and each fabricated film were determined from the DSC curves.

Film Transparency

The transparency of the films was determined by the measurement of the percentage transmittance with a UV–visible

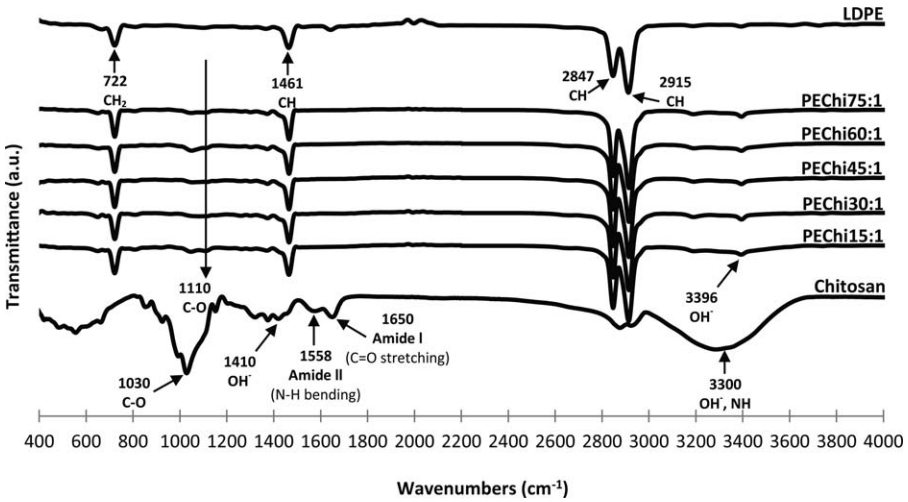

Figure 1. FTIR spectra of the chitosan powder, LDPE, and 80/20 PE/chitosan blend films with increasing length of compounding.

spectrophotometer (UV-3101PC, Shimadzu, Japan) according to ASTM D 1746.[17] We prepared the samples by cutting film into a rectangular piece before positioning it with a holder on the internal side of the spectrophotometer cell. A transmittance spectrum ranging from 220 to 800 nm was recorded for each sample. Three replicates of each film composition were measured, and the average values were recorded.

The transparency of the films was calculated with the following equation[18]:

$$\text{Transparency} = (\log T_{600})/b \quad (1)$$

where T_{600} is percentage transmittance of light at 600 nm and b is the thickness of the film (mm).

Field Emission Scanning Electron Microscopy (FESEM)

The morphology of the freeze-fractured cross sections and tensile fracture surfaces of the fabricated films was observed with FESEM (Hitachi S-4300 scanning electron microscope) at an accelerating voltage of 15 kV. Before examination, the fractured ends of the specimens were coated with gold sputtering to prevent electrostatic charging during the FESEM analysis.

Mechanical Properties

The mechanical properties of the blend films were measured according to ASTM D 882.[19] Film samples with dimensions of $15 \times 2\,cm^2$ were cut from the compression-molded films and preconditioned at $50 \pm 10\%$ relative humidity and $23 \pm 2\,^{\circ}C$ for at least 48 h before testing. The tensile tests were conducted in an Instron universal testing machine (Instron 3345 Tester, Instron, Norwood, MA) with a load cell of 500 N, a crosshead speed of 5 mm/min, and a gauge length of 11 mm. The tensile strength (TS), E_{break}, and Young's modulus (E) were determined. Five samples from each film were prepared, and the average values were reported.

b

b was measured with a handheld digital micrometer (Mitutoyo, Mitutoyo Corp., Japan). Measurements of b were taken randomly at 10 different locations of the film, and the mean b was calculated.

Statistical Analysis

Statistical analysis of the data was determined with an analysis of variance procedure. The length of compounding as a function of the l/d ratio was the treatment factor, and TS, E_{break}, and E were the response variables. Statistical differences among the experimental data were evaluated with a one-way analysis of variance followed by *post hoc* tests. All of the results were reported as mean values with standard deviation (Mean ± Standard deviation). In all analyses, differences were accepted as significant at $p \leq 0.05$.

RESULTS AND DISCUSSION

Chemical Bonds

The FTIR spectra of the individual polymers and PE/chitosan 80/20 blend films (PEChi15:1, PEChi30:1, PEChi45:1, PEChi60:1, and PEChi75:1) are shown in Figure 1. Chitosan powder displayed characteristic bands at 1650 and 1558 cm^{-1}; these corresponded to amide I, assigned to the stretching of the carbonyl (C═O) bond, and amide II, assigned to the bending vibrations of the N—H group, respectively. As the chitosan used for the fabrication of the films had a deacetylation degree of 75–85%, the peak at 1650 cm^{-1} represented the presence of acetylated amino groups of chitin. Both amide I and amide II bands decreased after blending with LDPE; this could have been due to the interactions between the amide groups of chitosan and the LDPE molecules, which formed a partially miscible structure. The broadest band observed between 3100 and 3500 cm^{-1} was attributed to the stretching vibrations of the hydroxyl (OH^-) and N—H groups in chitosan. The widening of the band was a result of the strong interaction between the OH^- groups from chitosan and the presence of moisture.[14] The absorption spectra at 1410 cm^{-1} also corresponded to the vibrations of OH^- groups. Moreover, the absorption band at 1030 cm^{-1} involved the stretching of C—O bonds and was distinctive of the saccharide structure of chitosan.

The characteristic bands of PE were detected at 2847 and 2951 cm^{-1} and were assigned to the stretching of symmetrical and asymmetrical hydrocarbon bonds, respectively. The absorption peak at 722 cm^{-1} was correlated with the rocking of

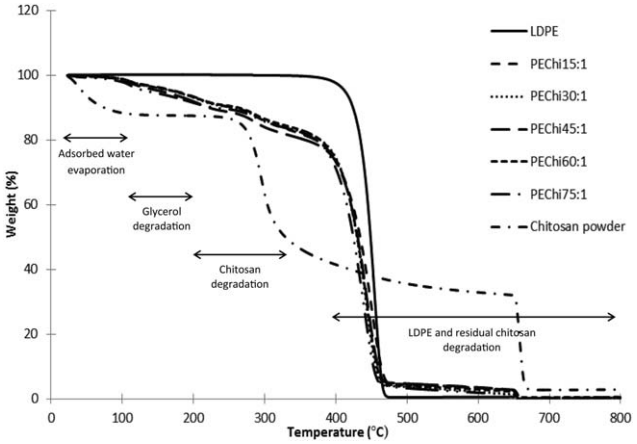

Figure 2. TG curves of the LDPE, chitosan powder, and 80/20 PE/chitosan blend films with increasing length of compounding.

methylene (CH_2) in —$(CH_2)_4$— units. The FTIR spectra of the PE/chitosan blend films also showed peaks at 1110 and 1461 cm^{-1} due to the stretching of C—O and bending of C—H bonds, respectively. A shift in the characteristic peak of C—O groups present in chitosan was detected in the spectra of the PE/chitosan films within the range 990–1110 cm^{-1}. In accordance with Wanchoo and Sharma,[20] within miscible blends, the presence of interactions between the chemical groups on dissimilar polymers would result in a shift in peak position of the bond spectra. Therefore, a shift in the peaks of the blend films demonstrated the interaction between chitosan and the LDPE matrix. We postulated that the interactions between LDPE and chitosan could be attributed to the similar chemical and geometrical linear structure of both polymers in the films.[21] On the other hand, the narrowing of the band between 3100 and 3500 cm^{-1} to the peak at 3396 cm^{-1} corresponding to the stretching vibrations of hydroxyl (OH^-) groups in the PE/chitosan films could be explained by the hydrophobic nature of LDPE as the matrix polymer in the blends.

However, as the analysis of the FTIR spectra revealed that no new bands were identified with respect to the spectra of the individual polymers, we deduced that no new chemical bonds were formed in the fabricated films.

Thermal Stability

TGA is important for the evaluation of films fabricated for packaging applications because the films might be subjected to intense heat treatment during preparation, processing, or preservation procedures. Figure 2 shows the thermogravimetry (TG) curves of the LDPE, chitosan powder, and PE/chitosan films. LDPE exhibited a single-stage degradation step that occurred within the temperature range 400–450 °C. Above 400 °C, the rapid mass loss of LDPE was due to the degradation of the LDPE residue into volatile products. As for chitosan powder, the initial weight loss around 100 °C resulted from the evaporation process of adsorbed water due to the hydrophilic nature of chitosan. The weight loss corresponding to residual water was determined to be 10% for the chitosan powder, and the onset of thermal degradation was at 230 °C. It is known that the presence of bound water always exists within chitosan even after it has been extensively dried.[22]

On the other hand, the TG curves of all of the PE/chitosan blend films showed four stages of degradation; these were observed to be the combined degradation steps of LDPE and plasticized chitosan. The initial weight loss corresponding to residual water ranged from 2 to 4% for the blend films. The second weight loss corresponding to the degradation of glycerol as the plasticizer in the blend films occurred in a one-step degradation at 250 °C. The third degradation stage, which ranged from 200 to 300 °C, was attributed to the complex thermal degradation pathway of chitosan and included the dehydration of the polysaccharide rings, pyrolytic depolymerization, and decomposition of the acetylated and deacetylated units of the chitosan molecules.[23] The fourth degradation step within the temperature range 400–450 °C and the final mass loss up to 700 °C were due to the decomposition of LDPE and residual chitosan decomposition reactions.[24] We noted that the degradation of LDPE was slightly faster with increasing length of compounding; this was possibly due to the effects of the thermomechanical treatment.

Despite the earlier initiation of LDPE degradation, all of the TG curves exhibited the same degradation stages, and the total weight losses recorded for all of the fabricated films were comparable to one another regardless of the length of compounding. Hence, TGA demonstrated that although the increasing length of compounding improved the miscibility of the blend films, the thermal stability of the films was not affected.

Film X_c

Table I presents the values of T_m, ΔH_f, and X_c of the LDPE and PE/chitosan films (PEChi15:1, PEChi30:1, PEChi45:1, PEChi60:1, and PEChi75:1). The X_c values of the films were calculated with the following relationship:

$$X_c = (\Delta H_f / \Delta H_{f^\circ}) \times 100\% \quad (2)$$

where ΔH_{f° is the heat of fusion of perfectly 100% crystalline LDPE, which was taken to be 277.1 J/g.[25]

LDPE exhibited a single T_m around 108 °C. The incorporation of chitosan with LDPE did not result in the formation of additional peaks, and the curves of all of the blend films displayed an endothermic single peak characteristic of LDPE around 108–109 °C. The observed insignificant differences in T_m with the incorporation of chitosan indicated that there were minimal hydrogen-bond interactions between the amine (NH_2) and

Table I. DSC Analysis of the LDPE and 80/20 PE/Chitosan Blend Films

Sample	T_m (°C)	ΔH_f (J/g)	X_c (%)
LDPE	108.5	74.5	26.9
PEChi15:1	107.9	56.1	20.2
PEChi30:1	108.9	63.3	22.8
PEChi45:1	108.3	63.7	23.0
PEChi60:1	108.2	71.7	25.9
PEChi75:1	108.3	71.9	25.9

Table II. Light Transmission Values of the LDPE and 80/20 PE/Chitosan Blend Films with Increasing Length of Compounding

Film	Light transmission (%)						Transparency: (log T_{600})/b
	300 nm	400 nm	500 nm	600 nm	700 nm	800 nm	
LDPE	106.3	86.6	86.5	86.7	87.0	87.2	6.5
PEChi15:1	11.3	41.5	74.3	83.8	86.2	86.8	6.2
PEChi30:1	12.8	43.4	75.0	83.9	86.2	86.9	6.5
PEChi45:1	10.2	38.8	73.0	83.1	85.7	86.6	6.5
PEChi60:1	8.7	34.7	70.2	82.3	85.6	86.6	6.5
PEChi75:1	8.6	36.8	71.8	82.5	85.3	86.2	6.5

hydroxyl (OH^-) groups of chitosan and the C—H groups of LDPE.[5,14] The results from the DSC curves were in accordance with the FTIR spectra.

It is shown in Table I that X_c of LDPE was markedly affected by the blending of chitosan with LDPE. X_c of LDPE was initially 26.9% but decreased to 20.3% with the incorporation of 20 wt % chitosan in the blend film (PEChi15:1). The lower X_c of the blend was due to the addition of chitosan, which inhibited the close packing of the LDPE chains as was also identified by other groups.[16,26]

However, as shown in Table I, it was evident from the larger values of X_c of PEChi60:1 and PEChi75:1 as compared to those of PEChi15:1, PEChi30:1, and PEChi45:1 that the X_c values of the blends increased with increasing length of compounding. The increases in the crystallization of the polymer blends with increasing length of compounding were attributed to the better dispersion of chitosan, which could act as the nucleating agent for polymer crystallization. With the same amount of chitosan (20 wt %) within all of the films, blends with a longer length of compounding exhibited higher ΔH_f and X_c values. The improvement in the X_c values of the blend films was due to the better interfacial interaction between chitosan and the LDPE matrix with increasing length of compounding; it enhanced the miscibility of the polymer blends. The improvement in the interfacial interaction of the polymer blends for PEChi60:1 and PEChi75:1 was also noticeable from the cross-sectional FESEM images, which revealed improvements in the adhesion, surface smoothness, and uniformity. A similar observation was reported for recycled PE/chitosan composites.[27]

Film Transparency

The transparency of the LDPE and all of the PE/chitosan films were analyzed through the measurement of the transmittance of the films in the range 220–800 nm. The film transparency was calculated on the basis of eq. (1). Table II presents the light transmission values and transparency at selected wavelengths from 300 to 800 nm for the films. In the UV-light region (220–400 nm), the LDPE film was clear and transparent, as indicated by the high transmittance value of 106.3% measured in the UV (300-nm) range. As noted from Table II, the transmittance of all of the PE/chitosan films decreased remarkably when chitosan was blended with LDPE. The measured transmittance indicated that although the LDPE films were highly transparent within the UV region without any barrier properties to UV light, the incorporation of chitosan in the film endowed it with barrier properties to UV light and could effectively prevent the penetration of UV into the packaged product. These results were in good agreement with those of Leceta *et al.*,[28] who reported that films based on chitosan were shown to have superior barrier properties to UV light in the UV region.

Despite the significant decrease in the transmittance values of the PE/chitosan films compared to LDPE in the UV-light region, it was interesting to note that the transmittance values of the LDPE and all PE/chitosan films were comparable in the visible-light region (400–800 nm). As observed from the light transmission at 600 nm, which is a wavelength typically used for the comparison of film transparency,[18,29,30] the obtained results indicate that the transparency of the films was not affected by the increase in the compounding length of the PE/chitosan blend. From the calculated film transparency values in Table II, we noted that regardless of the length of compounding, the transparency values of all of the PE/chitosan films were similar or identical and also corresponded to the transparency values of the LDPE films.

Film Morphology

FESEM micrographs of the cross-sectional surface of the PE/chitosan 80/20 films are shown in Figure 3. The micrographs revealed notable differences in the morphology as the length of compounding increased. The cross-sectional surface of the compression-molded PEChi15:1, PEChi30:1, and PEChi45:1 films exhibited a heterogeneous morphology [Figure 3(a,b)]. The coalescence of elliptical chitosan particles with voids at the interfaces between the LDPE matrix and chitosan were observed on the cross-sectional surface of the films; this indicated poor miscibility between LDPE and chitosan because of inadequate dispersion of chitosan and compatibilizer within the blend. The poor interfacial adhesion between the LDPE matrix and chitosan of the PEChi15:1 films thus resulted in weaker mechanical properties of the films, as reflected in the mechanical test results. The dispersion of chitosan with LDPE matrix improved with longer length of compounding. At the same time, the incidences of large voids embedded within the cross section of the blend films decreased when the length of compounding was longer [Figure 3(b)]; this corresponded to an improvement in the TS and E_{break} values of the films.

Increases in the length of compounding allowed for a better dispersion of chitosan in LDPE, as evidenced by the improved

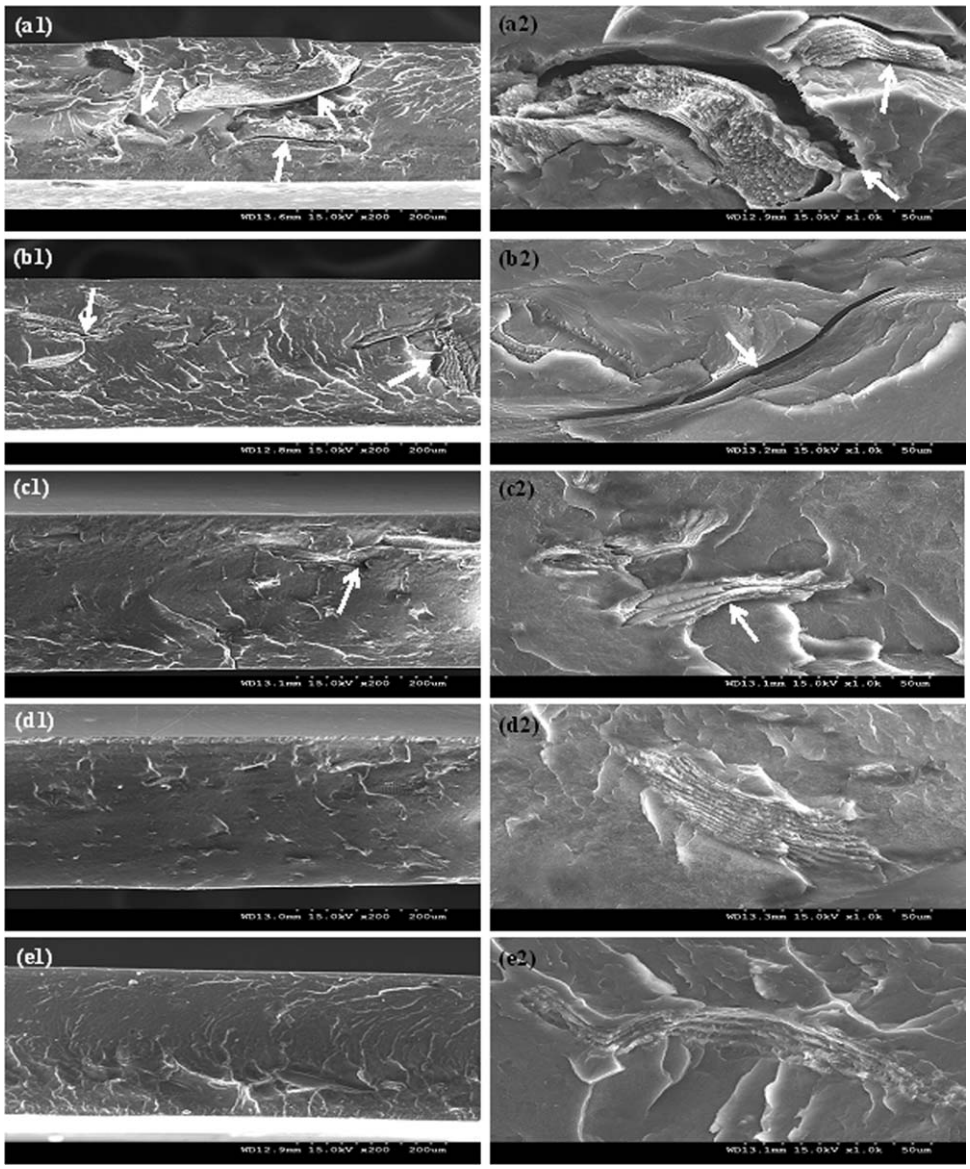

Figure 3. FESEM images of the cross-sectional surfaces of the 80/20 PE/chitosan blend films with increasing length of compounding: (a) PEChi15:1, (b) PEChi30:1, (c) PEChi45:1, (d) PEChi60:1, and (e) PEChi75:1. The arrows in the FESEM images indicate the locations of voids between the LDPE matrix and chitosan.

surface smoothness and uniformity of the cross-sectional morphologies for the PEChi60:1 and PEChi75:1 films [Figure 3(d,e)]. An enhancement in the interfacial adhesion between the LDPE matrix and chitosan particles was also apparent with minimal voids. The results obtained from the film morphological analysis support the increase in TS and E_{break} values recorded from the mechanical test results.

FESEM micrographs of the tensile fracture surface for the PEChi15:1, PEChi30:1, PEChi45:1, PEChi60:1, and PEChi75:1 films are shown in Figure 4. Similar to the cross-sectional surfaces of the films, the micrographs showed visible differences in the morphologies of the fracture surfaces. Micrographs of the PEChi15:1, PEChi30:1, and PEChi45:1 films [Figure 4(a–c)] revealed extensive tearing of the LDPE matrix, with clearly distinguishable chitosan particles embedded within the matrix. In addition to the observable chitosan particles on the fracture surface of PEChi15:1, PEChi30:1, and PEChi45:1, voids representing the detachment of the chitosan particles were also noticeable. The fracture surface morphology of PEChi15:1 [Figure 4(a)] appeared to be the roughest and contained the largest voids and chitosan particles; this supported the lowest TS and E_{break} values recorded for the mechanical testing. Because of the poor adhesion between the chitosan and LDPE matrix, which caused the separation of the polymers during mechanical testing, the TS and E_{break} of PEChi15:1, PEChi30:1, and PEChi45:1 films were weaker.

However, with an increase in the length of compounding times for the PEChi60:1 and PEChi75:1 films [Figure 4(d,e)], the morphology of the fracture surface became apparently smoother, with little tearing of the LDPE polymer. The

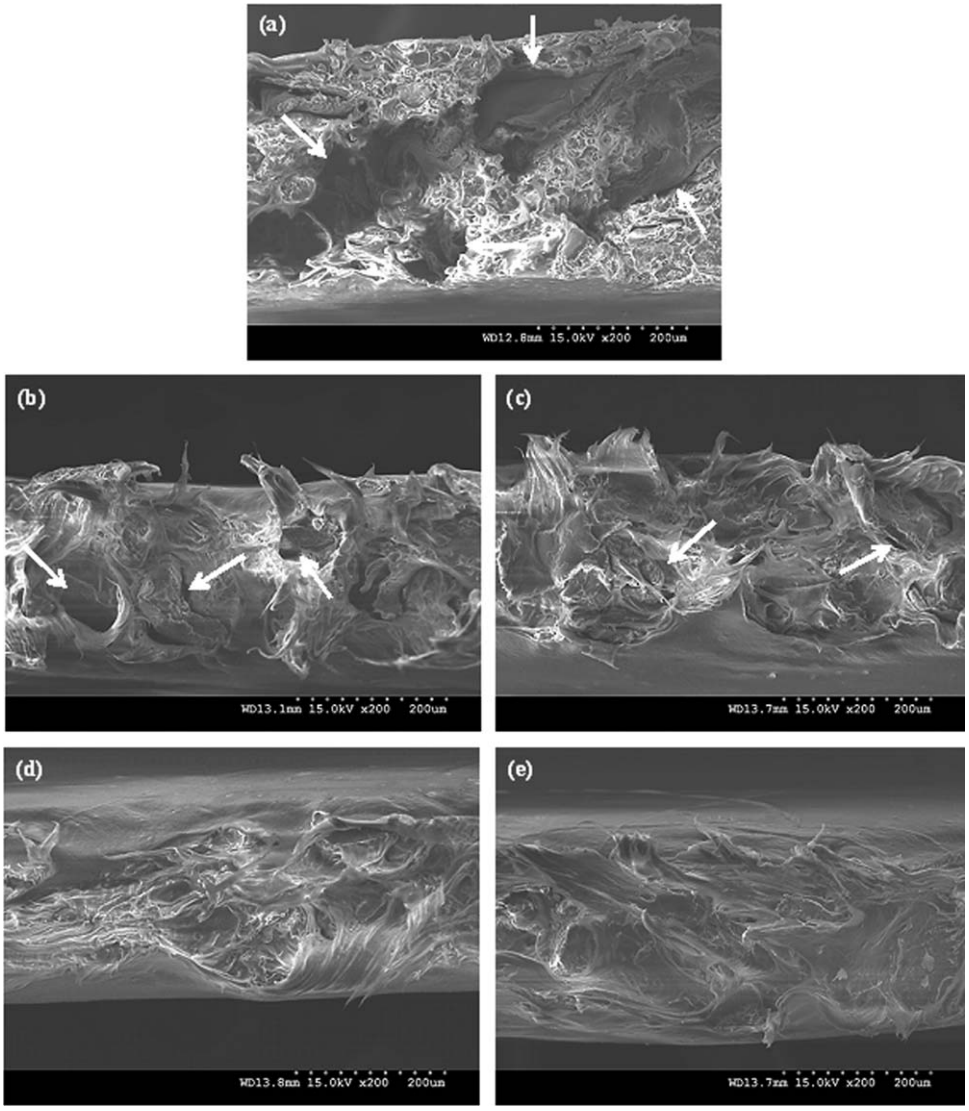

Figure 4. FESEM images of the tensile fracture surfaces of the 80/20 PE/chitosan blend films with increasing length of compounding: (a) PEChi15:1, (b) PEChi30:1, (c) PEChi45:1, (d) PEChi60:1, and (e) PEChi75:1. The arrows in the FESEM images indicate the locations of voids due to the detachment of chitosan particles.

separation of chitosan particles from the LDPE matrix was no longer visible, and better adhesion between chitosan and the matrix was evident. The increasing length of compounding improved the blending and miscibility of the PE/chitosan blend films and, consequently, resulted in higher mechanical properties in the PEChi60:1 and PEChi75:1 films.

Mechanical Properties of the PE/Chitosan Blend Films

Table III presents the values of TS, E_{break}, and E of the blend films as a function of the l/d ratio used for the compounding of the polymer blends. Generally, we observed that with increasing length of compounding, both the TS and E_{break} values of the films displayed an increasing trend, whereas there was a decrease in the E values of the films.

As shown in Table III, TS displayed a significant increase of approximately 25% ($p < 0.05$) when the l/d ratio of the compounder was greater than 30:1 compared to the PEChi15:1 films. A twofold increase in the E_{break} value of the fabricated films was also noted when the length of compounding was longer than $l/d = 45:1$. When the compounding length was short, the TS and E_{break} values were low because of the ineffective blending and poor dispersion of chitosan in the LDPE matrix, as observed from the coalescence of chitosan particles on the cross-sectional surfaces of the PEChi15:1, PEChi30:1, and PEChi45:1 blend films [Figure 3(a–c)]. Large chitosan particles resided in the matrix as flaws; this reduced the strength of the blend films. Studies have indicated that mechanical performance is directly affected by the quality of dispersion and interfacial adhesion between components.[31,32]

Thus, with increasing length of compounding, the more extensive dispersion of chitosan within the matrix and more uniform distribution of compatibilizer at the interfaces between the matrix polymer and chitosan enhanced the overall mechanical performance of the blend films. A more uniform distribution of

Table III. Mechanical Properties of the 80/20 PE/Chitosan Blend Films

Sample	*b* (mm)	TS (MPa)	E_{break} (%)	*E* (MPa)
PEChi15:1	$0.312 \pm 0.008^{a,b,c,d}$	$7.5 \pm 0.6^{a,b,c,d}$	$7.4 \pm 0.9^{a,b,c,d}$	$245.4 \pm 11.6^{a,b,c,d}$
PEChi30:1	0.297 ± 0.007	9.4 ± 0.4^{e}	$12.6 \pm 2.0^{e,g}$	215.0 ± 13.8
PEChi45:1	0.295 ± 0.005	9.6 ± 0.3^{f}	$15.6 \pm 3.4^{f,h}$	208.9 ± 14.1
PEChi60:1	0.295 ± 0.007	10.1 ± 0.3	20.3 ± 1.6	201.8 ± 11.7
PEChi75:1	0.297 ± 0.007	9.9 ± 0.6	17.0 ± 1.6	201.4 ± 15.1

The values are presented as means and standard deviations (*n* for *b* = 10, *n* for TS = 5, *n* for E_{break} = 5, *n* for *E* = 5).
[a] $p < 0.05$ when comparing PEChi15:1 to PEChi30:1.
[b] $p < 0.05$ when comparing PEChi15:1 to PEChi45:1.
[c] $p < 0.05$ when comparing PEChi15:1 to PEChi60:1.
[d] $p < 0.05$ when comparing PEChi15:1 to PEChi75:1.
[e] $p < 0.05$ when comparing PEChi30:1 to PEChi60:1.
[f] $p < 0.05$ when comparing PEChi45:1 to PEChi60:1.
[g] $p < 0.05$ when comparing PEChi30:1 to PEChi75:1.
[h] $p < 0.05$ when comparing PEChi45:1 to PEChi75:1.

stress transfer from the LDPE matrix to chitosan at the interfaces resulted in an increase in TS. The effects of pulverization and the higher degree of distribution of chitosan in the matrix contributed to the steady increase in the values of E_{break}. For all of the fabricated films, it was evident that the improvement in the mechanical properties also tended to coincide with the results from the FESEM images, as with the increasing length of compounding, the morphology of the cross section of the films revealed better miscibility and interfacial adhesion between the LDPE and chitosan, with a reduction in the incidences of voids. Similar results were also reported in studies involving polystyrene and polypropylene composites.[31,33,34] Low values of TS and E_{break} were recorded as a result of ineffective mixing and poor dispersion of fillers within the polymer matrices, and the mechanical properties improved with the enhancement in the dispersion of fillers and homogeneity in the matrixes. On the other hand, *E* displayed a decreasing trend with increasing compounding length; this was attributed to the increased dispersion of chitosan in the blend films.[35]

However, as the length of compounding increased, TS and E_{break} increased and reached a maximum value at an *l*/*d* ratio of 60:1; this subsequently levelled off at a longer compounding length. The highest TS and E_{break} values were both recorded for the PEChi60:1 films. The TS value of 10.1 ± 0.3 MPa achieved for the PEChi60:1 films containing 20 wt % chitosan was promising, as it reflected an improvement from the TS value of compression-molded PE films with 20 wt % chitosan reported by Sunilkumar *et al.*[21] at 7.8 ± 0.4 MPa. Furthermore, the TS value of 10.1 ± 0.3 MPa recorded for the PEChi60:1 films was also comparable to the TS of the LDPE films at 8.2 ± 0.7 MPa measured experimentally.

It has been reported that tensile loading on ternary blends has the effect of causing the failure of the films at the interface between PE and chitosan.[3] Hence, the increasing length of compounding of the PE/chitosan blend improved the interaction between the interfaces of PE and chitosan and enhanced the miscibility of both polymers; this resulted in an increase in the mechanical properties of the blend films.

CONCLUSIONS

Chitosan, a biodegradable and antimicrobial natural polysaccharide was successfully blended with LDPE via compounding and fabricated into films by compression molding. The length of compounding had a direct influence on the miscibility of the blends, and this affected the interfacial adherence and mechanical properties of the resulting fabricated films.

FTIR analysis validated the interactions between LDPE and chitosan in the formation of a miscible structure. It was evident that the improvement in interfacial interactions between LDPE and chitosan also tended to coincide with the results from DSC by the way the X_c values of the blend films increased with increasing compounding length. Although the degradation of LDPE was noted to be initiated earlier with increasing length of compounding, the results of thermal analysis demonstrate that the increase in the length of compounding did not affect the thermal stability of the compression-molded PE/chitosan blend films, and all of the films exhibited good thermal stability. The transparency of the PE/chitosan films was also comparable to that of the LDPE films.

FESEM micrographs of the PE/chitosan blend films revealed better interfacial adhesion between the polymers and enhanced uniformity in the morphology with increasing length of compounding. Furthermore, results from the mechanical tests generally show that both the TS and E_{break} values of the PE/chitosan films increased with increasing length of compounding. With 20 wt % chitosan, the optimum length of compounding was at an *l*/*d* ratio of 60:1, where both TS and E_{break} recorded their highest values, and the TS of the films was comparable to that of commonly used synthetic LDPE films. The improvement in the mechanical properties of the films was attributed to the better dispersion of chitosan and compatibilizer, which was facilitated by the longer compounding length. These led to a higher degree of miscibility within the PE/chitosan films and, consequently, allowed for a more uniform distribution of stress transfer from the PE matrix to chitosan at the interface.

Therefore, biodegradable PE/chitosan blend films, with good miscibility and satisfactory structural and mechanical properties,

have the potential to be used as environmentally friendly packaging materials in food technology applications.

ACKNOWLEDGMENTS

The authors thank the National University of Singapore for awarding a National University of Singapore Research Scholarship to one of the authors (Y.M.T.).

REFERENCES

1. Vasile, C.; Darie, R. N.; Sdrobis, A.; Pâslaru, E.; Pricope, G.; Baklavaridis, A.; Munteanu, S. B.; Zuburtikudis, I. *Cell Chem. Technol.* **2014**, *48*, 325.
2. Orhan, Y.; Hrenovic, J.; Buyukgungor, H. *Acta Chim. Slov.* **2004**, *51*, 579.
3. Quiroz-Castillo, J. M.; Rodríguez-Félix, D. E.; Grijalva-Monteverde, H.; Del, C. T.; Plascencia-Jatomea, M.; Rodríquez-Félix, F.; Herrera-Franco, P. J. *Carbohydr. Polym.* **2014**, *101*, 1094.
4. Rogovina, S. Z.; Alexanyan, C. V.; Prut, E. V. *J. Appl. Polym. Sci.* **2011**, *121*, 1850.
5. Correlo, V. M.; Boesel, L. F.; Bhattacharya, M.; Mano, J. F.; Neves, N. M.; Reis, R. L. *Mater. Sci. Eng. A* **2005**, *403*, 57.
6. Ermolovich, O. A.; Makarevich, A. V. *Russ. J. Appl. Chem.* **2006**, *79*, 1526.
7. Clarinval, A. M.; Halleux, J. In Biodegradable Polymers for Industrial Applications; Smith, R., Ed.; Woodhead: Cambridge, United Kingdom, **2005**; p 3.
8. Kong, M.; Chen, X. G.; Xing, K.; Park, H. J. *Int. J. Food Microbiol.* **2010**, *144*, 51.
9. Park, J. H.; Saravanakumar, G.; Kwangmeyung, K.; Kwon, I. C. *Adv. Drug Delivery Rev.* **2010**, *62*, 28.
10. Li, J.; Zivanovic, S.; Davidson, P. M.; Kit, K. *Carbohydr. Polym.* **2010**, *79*, 786.
11. Rodríguez-Félix, D. E.; Quiroz-Castillo, J. M.; Grijalva-Monteverde, H.; Castillo-Castro, T. D.; Burruel-Ibarra, S. E.; Rodríguez-Félix, F.; Madera-Santana, T.; Cabanillas, R. E.; Herrera-Franco, P. J. *J. Appl. Polym. Sci.* **2014**, *131*, DOI: 10.1002/app.41045.
12. Del Castillo-Castro, T.; Castillo-Ortega, M. M.; Herrera-Franco, P. J.; Rodríguez-Félix, D. E. *J. Appl. Polym. Sci.* **2011**, *119*, 2895.
13. Akopova, T. A.; Vladimirov, L. V.; Zhorin, V. A.; Zelenetskii, A. N. *Polym. Sci. Ser. B* **2009**, *51*, 124.
14. Martínez-Camacho, A. P.; Cortez-Rocha, M. O.; Graciano-Verdugo, A. A.; Rodríguez-Félix, F.; Castillo-Ortega, M. M.; Burgos-Hernández, A.; Ezquerra-Brauer, J. M.; Plascencia-Jatomea, M. *Carbohydr. Polym.* **2013**, *91*, 666.
15. Berlin, A. A.; Henrici-Olive, G.; Olive, S. Principles of Polymer Composites; Springer-Verlag: New York, **1986**; Vol. *10*.
16. Vasile, C.; Darie, R. N.; Cheaburu-Yilmaz, C. N.; Pricope, G.; Bračič, M.; Pamfil, D.; Hitruc, G. E.; Duraccio, D. *Compos. B* **2013**, *55*, 314.
17. ASTM International. Standard Test Method for Transparency of Plastic Sheeting; ASTM D 1746-09; ASTM International: West Conshohocken, PA, **2009**.
18. Han, J. H.; Floros, J. D. *J. Plast. Film Sheeting* **1997**, *13*, 287.
19. ASTM International. Standard Test Method for Tensile Properties of Thin Plastic Sheeting; ASTM D 882-12; ASTM International: West Conshohocken, PA, **2012**.
20. Wanchoo, R. K.; Sharma, P. K. *Eur. Polym. J.* **2003**, *39*, 1481.
21. Sunilkumar, M.; Francis, T.; Thachil, E. T.; Sujith, A. *Chem. Eng. J.* **2012**, *204*, 114.
22. Souza, B. W. S.; Cerqueira, M. A.; Martins, J. T.; Casariego, A.; Teixeira, J. A.; Vicente, A. A. *Food Hydrocolloids* **2010**, *24*, 330.
23. Kurek, M.; Brachais, C.; Nguimjeu, C. M.; Bonnotte, A.; Galić, A.; Couvercelle, J.; Debeaufort, F. *Polym. Degrad. Stabil.* **2012**, *97*, 1232.
24. Wanjun, T.; Cunxin, W.; Donghua, C. *Polym. Degrad. Stabil.* **2005**, *87*, 389.
25. Bandrup, J.; Immergut, E. H. Polymer Handbook, 2nd ed.; Wiley: New York, **1975**.
26. Mir, S.; Yasin, T.; Halley, P. J.; Siddiqi, H. M.; Nicholson, T. *Carbohydr. Polym.* **2011**, *83*, 414.
27. Salmah, H.; Azieyanti, A. N. *J. Reinf. Plast. Compos.* **2011**, *30*, 195.
28. Leceta, I.; Guerrero, P.; de la Caba, K. *Carbohydr. Polym.* **2013**, *93*, 339.
29. Fang, Y.; Tung, M. A.; Britt, I. J.; Yada, S.; Dalgleish, D. G. *J. Food Sci.* **2002**, *67*,188.
30. Zhang, Y.; Han, J. H. *J. Food Sci.* **2006**, *71*, 6, E253.
31. Joseph, P. V.; Joseph, K.; Thomas, S. *Compos. Sci. Technol.* **1999**, *59*, 1625.
32. Jollands, M.; Gupta, R. K. *J. Appl. Polym. Sci.* **2010**, *118*, 1489.
33. Maldas, D.; Kokta, B. V. *Int. J. Polym. Mater.* **1990**, *14*, 165.
34. Takase, S.; Shiraishi, N. *J. Appl. Polym. Sci.* **1989**, *37*, 645.
35. Lu, J. Z.; Wu, Q.; Negulescu, I. I. *J. Appl. Polym. Sci.* **2004**, *93*, 2570.